Lukanidin E, Kozlova EN. Sensory neurite outgrowth on white matter astrocytes is influenced by intracellular and extracellular S100A4 protein. J. Neurosci. Res. 2006; 83:619-626.
5. Koshikawa N, Maejima C, Miyazaki K, Nakagawara A, Takenaga K. Hypoxia selects for high-metastatic Lewis lung carcinoma cells overexpressing Mcl-1 and exhibiting reduced apoptotic potential in solid tumors. Oncogene 2006; 25:917-928.
6. Takenaga K, Kozlova EN. The role of intra-cellular S100A4 for migration of rat astro-cytes. Glia. 2006; 53:313-321.

H. 知的財産権の出願・登録状況

1. 特許取得

なし

2. 実用新案登録

なし

3. その他

なし

厚生労働科学研究費補助金（第３次対がん総合戦略研究事業）
平成 18 年度　分担研究報告書

マウスモデルを用いた個体発生と発がんに関する遺伝子の解析

分担研究者　古関　明彦　独立行政法人理化学研究所免疫器官形成研究グループグループディレクター

研究要旨　ほ乳類ポリコム群は、Ink4a/p53 経路に対して抑制的に作用して細胞老化を制御することが遺伝学的に示されている。この抑制は、ポリコム群複合体の Ink4a 遺伝子座への直接結合を介しているを今まで示してきた。さらに、ポリコム群複合体の発現が、その結合タンパクである Pcl2 によって制御されることも明らかにしてきた。今回、Pcl 2 によるポリコム群タンパクの発現制御が、翻訳調節を介したメカニズムであることを新たに示した。これらの結果は、細胞老化の制御には、ボトルネックとなるタンパク群の翻訳調節が寄与している可能性を示唆している。今後は、この翻訳調節の分子メカニズムを明らかにすることで、発がんに寄与する分子サーキットの新たな側面を切り開きうる。

A.　研究目的

ほ乳類ポリコム群は、Ink4a/p53 経路に対して抑制的に機能することが遺伝学的に示されている。さらに、この経路は一部の白血病では腫瘍幹細胞において重要な機能を果たすことも示唆されている。本研究では、ポリコム群タンパクの機能発現メカニズムを明らかにするために、ポリコム群結合タンパク群による Ink4a 遺伝子座の発現制御メカニズムを解析する。

B.　研究方法

昨年度までに、ポリコム群複合体は、MEF において Ink4a 遺伝子座へ直接結合することにより、Ink4a 遺伝子座の転写抑制に寄与することを示した。さらにポリコム複合体に結合するタンパクである Polycomblike 2 （Pcl2）は、ポリコム群タンパクの発現を制御することにより、Ink4a 発現を制御することを Pcl2 欠損と他のポリコム群遺伝子の欠損マウスを交配する実験から明らかにした。Pcl2 は、ポリコム群複合体の発現量を低下させる機能を持つ、すなわち、Ink4a 遺伝子産物の発現を増強するがん抑制遺伝子として機能しうる可能性を示してきた。本年度は、Pcl2 がどのようにポリコム群複合体の発現を制御するのか、そのメカニズムを明らかにするために、まず Pcl2 が構成しうるタンパク複合体を精製し、それに基づいて Pcl2 は翻訳制御に寄与するという作業仮説を考えた。その仮説を検証するために、Pcl2 欠損 MEF と野生型 MEF の間で、ポリコム群をコードする転写産物の翻訳頻度の比較を試みた。

C.　研究結果

ポリコム群タンパクである Mel18 に結合するタンパクとして新たに同定したショウジョウバエ・ポリコムライクのホモログである Pcl2 は、TUDOR ドメインとふたつの PHD フィンガーを有している。TUDOR ドメインは、メチル化リシンの結合モチーフとしてだけでなく、RNA 結合ドメインとしても機能しうることが、いくつかの TUDOR ドメインにおいて示されている。実際、Pcl2 の TUDOR ドメインの構造を NMR によって解いてみると、RNA 結合に適したポケットを有していることが明らかになった。Pcl2 が、RNA 結合あるいは RNA メタボリズムに寄与する可能性を検討するために、Pcl2 に結合するタンパク質群の中に、これらの過程に寄与するタンパ

ク質が濃縮されてくるかを解析した。Pcl2 に TAP タグを付加して 293T 細胞に一過性に発現させ、Pcl2 結合タンパクをプルダウンした。その中には、リボソームを構成するタンパク群、RNA ヘリケース群、RNA 結合タンパク、各種核小体タンパクなど翻訳に寄与しうるタンパクが有意に免疫共沈降されてきた。そこで、実際に翻訳制御に寄与しうるか否かを、Pcl2 を欠損した MEF を用いて解析した。野生型及び Pcl2 欠損 MEF よりポリソーム画分を抽出し、蔗糖濃度勾配法によって比重に従って分画した。この方法により，翻訳が活発におこっているポリソームとおこっていないポリソームとを分画しうる。これらの分画におけるポリコム群をコードする mRNA の分配をノザン法によって解析すると、Ring1B、Phc1、Scmh1、Bmi1 は Pcl2 欠損 MEF では野生型に比べて、非翻訳画分において顕著に減少していることが示された。このことから、Pcl2 によるポリコム群タンパクの発現制御は、ポリコム群タンパクの翻訳調節を含むことが明らかになった。以上の結果は、Pcl2 はポリコム群の翻訳調節を介してがん抑制因子として機能することを示している。

D. 考察

同様の翻訳調節は、同じく細胞老化に寄与する p53 においても報告されている(Takagi et al., Cell 123, 49-63)。ここでは、核小体タンパクである Nucleolin とリボソームの構成成分が、p53 の 5'-非翻訳領域に結合して翻訳調節を行うことが示されている。Nucleolin とリボソームの構成成分のいずれも Pcl2 に結合するタンパクとして同定されている（古関・未発表データ)。さらに、Pcl2 は、p53 依存的な転写活性化をひき起こしうる（古関・未発表データ)。これらの結果は、細胞老化の制御には、ボトルネックとなるタンパク群の翻訳調節が寄与している可能性を示唆している。今後は、この翻訳調節の分子メカニズムを明らかにすることで、発がんに寄与する分子サーキットの新たな側面を切り開きうる。

E. 結論

新規ポリコム群タンパク Pcl2 は、ポリコム群複合体の翻訳調節を介して Ink4a 遺伝子座の発現制御を行うがん抑制遺伝子の新たな候補であることを示した。

G. 研究発表

1. Isono, K., Nemoto, K., Li,Y., Takada, Y., Suzuki, R., Katsuki, M., Nakagawara, A., and Koseki, H., Overlapping roles for homeodomain-interacting protein kinases Hipk1 and Hipk2 in the mediation of cell growth in response to morphogenetic and genotoxic signals Mol. Cell. Biol. (2006) 26(7):2758-2771.
2. Takano-Maruyama M, Hase K, Fukamachi H, Kato Y, Koseki H, Ohno H.,"Foxl1-deficient mice exhibit aberrant epithelial cell positioning due to dysregulated EphB/EphrinB expression in the small intestine Am J Physiol Gastrointest Liver Physiol. (2006) 291(1):G163-170.
3. Blewitt M.E., Vickaryous N K. , Paldi A., Koseki H, Whitelaw E, "Dynamic reprogramming of DNA methylation at an epigenetically sensitive allele in mice PLoS Genet. (2006);2(4):e49.
4. Lee T.I., Jenner R.G.., Boyer L.A., Guenther M.G.., Levine S.S., Kumar R.M., Chevalier B, Johnstone S.E., Cole M. F., Isono K, Koseki H, Fuchikami T, Abe K, Murray H.L., Zucker J.P., Yuan B, Bell G.W., Herbolsheimer E, Hannett N.M., Sun K, Odom D.T., Volkert T.L., Bartel D.P, Melton D.A., Gifford D.K., Jaenisch R, Young R.A. (2006) Control of Developmental Regulators by Polycomb in Human Embryonic Stem Cells Cell 125(2):301-313.
5. Fujimura Y, Isono K, Vidal M, Endoh M, Kajita H, Mizutani-Koseki Y, Takihara Y, van Lohuizen M, Otte A, Jenuwein T, Deschamps J, Koseki H. (2006) Distinct roles of Polycomb group gene products between transcriptionally repressed and active domains

of Hoxb8 Development 133:2371-2381

6. Aikawa Y, Nguyen LA, Isono K, Takakura N, Tagata Y, Schmitz ML, Koseki H, Kitabayashi I. (2006) Roles of HIPK1 and HIPK2 in AML1- and p300-dependent transcription, hematopoiesis and blood vessel formation. EMBOJ. 25(17):3955-3965.
7. Jorgensen HF, Giadrossi S, Casanova M, Endoh M, Koseki H, Brockdorff N, Fisher AG. (2006) Stem cells primed for action: polycomb repressive complexes restrain the expression of lineage-specific regulators in embryonic stemcells. Cell Cycle. 5(13):1411-144.
8. Sato T, Endoh M, Yoshida H, Yasuo S, Katsuno T, Saito Y, Isono K, Koseki H. (2006) Mammalian Polycomb complexes are required for Peyer's patch development by regulating lymphoid cell proliferation. Gene. Sep 1;379:166-174. Epub 2006 May 25.
9. Nakayama M, Iida M, Koseki H, Ohara O. (2006) A gene-targeting approach for functional characterization of KIAA genes encoding extremely large proteins. FASEB J. Aug;20(10):1718-20. Epub 2006 Jun 28.
10. Schoeftner S, Sengupta AK, Kubicek S, Mechtler K, Spahn L, Koseki H, Jenuwein T, Wutz A. (2006) Recruitment of PRC1 function at the initiation of X inactivation independent of PRC2 and silencing. EMBO J. 25:3110-3122.
11. Nakajima Y, Morimoto M, Takahashi Y, Koseki H, Saga Y. (2006) Identification of Epha4 enhancer required for segmental expression and the regulation by Mesp2. Development 133:2517-2525.
12. Hosokawa H, Kimura MY, Shinnakasu R, Suzuki A, Miki T, Koseki H, van Lohuizen M, Yamashita M, Nakayama T. (2006) Regulation of Th2 Cell Development by Polycomb Group Gene bmi-1 through the Stabilization of GATA3. J Immunol. 177:7656-64.
13. Ogino J, Sakurai K, Yoshiwara K, Suzuki Y, Ishizuka N, Seki N, Suzuki Y, Koseki H, Shirasawa T, Hashimoto N, Yagui K, Saito Y. (2006) Insulin resistance and increased pancreatic beta-cell proliferation in mice expressing a mutant insulin receptor (P1195L). J Endocrinol. 190(3):739-747.
14. Nakajima M, Ogawa M, Shimoda Y, Koseki H, Shirasawa T, Furukawa K. (2007) Accelerated acquisition of permeability barrier function in the skin of presenilin-1-deficient embryos. Arch Dermatol Res. 298:339-345.
15. Matsuki Y, Ohmura-Hoshino M, Goto E, Aoki M, Mito-Yoshida M, Uematsu M, Hasegawa T, Koseki H, Ohara O, Nakayama M, Toyooka K, Matsuoka K, Hotta H, Yamamoto A, Ishido S. (2007) Novel regulation of MHC class II function in B cells. EMBO J. 26:846-854.
16. Takada Y, Isono K, Shinga J, Turner JM, Kitamura H, Ohara O, Watanabe G, Singh PB, Kamijo T, Jenuwein T, Burgoyne PS, Koseki H. (2007) Mammalian Polycomb Scmh1 mediates exclusion of Polycomb complexes from the XY body in the pachytene spermatocytes. Development 134:579-590.
17. Negishi M, Saraya A, Miyagi S, Nagao K, Inagaki Y, Nishikawa M, Tajima S, Koseki H, Tsuda H, Takasaki Y, Nakauchi H, Iwama A. (2007) Bmi1 cooperates with Dnmt1-associated protein 1 in gene silencing. Biochem Biophys Res Commun. 353:992-998.
18. Dietrich N, Bracken AP, Trinh E, Schjerling CK, Koseki H, Rappsilber J, Helin K, Hansen KH. (2007) Bypass of senescence by the polycomb group protein CBX8 through direct binding to the INK4A-ARF locus. EMBO J. 2007 Mar 1; [Epub ahead of print]
19. Kato Y, Koseki H, Vidal M, Nakauchi H, Iwama A. (2007) Unique composition of polycomb repressive complex 1 in hematopoietic stem cells. Int J Hematol. 85:179-181.

H. 知的財産権の出願・登録状況

古関明彦が出願者、発明者に含まれているもの

発明の名称：クローン哺乳動物の作成方法
出願日：２００５年６月１７日
公開日：２００６年３月３０日
出願人：独立行政法人理化学研究所
出願番号：特許出願２００５－１７７９９８
公開番号：特許公開２００６－８１５４２

発明者：若尾 宏 外４名

特許公開 2006－109742 インスリン受容体自己リン酸化不全に関連する遺伝子の検出法
出願日: ２００４年１０月１４日
公開番号: 特許公開２００６－１０９７４２
公開日: ２００６年４月２７日
出願人: 株式会社サイメディア外３名
発明者: 白澤 卓二 外３名

Ⅲ．研究成果の刊行に関する一覧表

研究成果の刊行に関する一覧表

雑誌

発表者氏名	論文タイトル名	発表誌名	巻号	ページ	出版年
Koshikawa N, Maejima C, Miyazaki K, Nakagawara A, Takenaga K.	Hypoxia selects for high-metastatic Lewis lung carcinoma cells overexpressing Mcl-1 and exhibiting reduced apoptotic potential in solid tumors.	Oncogene	25	917-928	2006
Kaneko Y, Kobayashi H, Watanabe N, Tomioka N, Nakagawara A.	Biology of neuroblastomas that were found by mass screening at 6 months of age in Japan.	Pediatr. Blood Cancer	46	285-291	2006
Inamori K, Gu J, Ohira M, Kawasaki A, Nakamura Y, Nakagawa T, Kondo A, Miyoshi E, Nakagawara A, Taniguchi N.	High expression of N-acetylglucosaminyltransferase V in favorable neuroblastomas: Involvement of its effect on apoptosis.	FEBS Lett.	580	627-632	2006
Isono K, Nemoto K, Li Y, Takada Y, Suzuki R, Katsuki M, Nakagawara A, Koseki H.	Overlapping roles for homeodomain-interacting protein kinases Hipk1 and Hipk2 in the mediation of cell growth in response to morphogenetic and genotoxic signals.	Moll. Cell. Biol.	26	2758-2771	2006
Machida T, Fujita T, Ooo M L, Ohira M, Isogai E, Mihara M, Hirato J, Tomotsune D, Hirata T, Fujimori M, Adachi W, Nakagawara A.	Increased expression of pro-apoptotic *BMCC1*, a novel gene with the *BNIP2* and *Cdc42GAP* homology (BCH) domain, is associated with poor prognosis in human neuroblastomas.	Oncogene	25	1931-1942	2006
Niizuma H, Nakamura Y, Ozaki T, Ohira M, Isogai E, Kageyama H, Imaizumi M, Nakagawara A.	Bcl-2 is a key regulator for the retinoic acid-induced apoptotic cell death in neuroblastoma.	Oncogene	25	5046-5055	2006
Chen H, Suzuki M, Nakamura Y, Ohira M, Ando S, Iida T., Nakajima T, Nakagawara A, Kimura H.	Aberrant methylation of RASGRF2 and RASSF1A in human non-small cell lung cancer.	Oncol. Rep.	15	1281-1285	2006

Sang M, Li Y, Ozaki T, Ono S, Ando K, Yamamoto H, Koda T, Geng C, Nakagawara A.	p73-dependent induction of 14-3-3σ increases the chemo-sensitivity of drug-resistant human breast cancers.	Biochem. Biophys. Res. Commun.	347	327-333	2006
Hayashi S, Ozaki T, Yoshida K, Hosoda M, Todo S, Akiyama S, Nakagawara A.	p73 and MDM2 confer the resistance of epidermoid carcinoma to cisplatin by blocking p53.	Biochem. Biophys. Res. Commun.	347	60-66	2006
Ozaki T, Li Y, Kikuchi H, Tomita T, Iwatsubo T, Nakagawara A.	The intracellular domain of the amyloid precursor protein (AICD) enhances the p53-mediated apoptosis.	Biochem. Biophys. Res. Commun.	351	57-63	2006
Kikuchi H, Ozaki T, Furuya K, Hanamoto T, Nakanishi M, Yamamoto H, Yoshida K, Todo S, Nakagawara A.	NF-kB regulates the stability and activity of p73 by inducing its proteolytic degradation through a ubiquitin-dependent proteasome pathway.	Oncogene	25	7608-7617	2006
Okahara F, Itoh K, Nakagawara A, Murakami M, Kanaho Y, Maehara T.	Critical role of PICT1, a tumor suppressor candidate, in phosphatidylinositol 3,4,5-triphosphate signals and tumorigenic transformation.	Mol. Biol. Cell	17	4888-4895	2006
Takenaga K, Kozlova EN.	The role of intracellular S100A4 for migration of rat astrocytes.	Glia	53	313-321	2006
Ito A, Koshikawa N, Mochizuki S., Omura K, Takenaga K.	Hypoxia-inducible factor-1 mediates the expression of DNA polymerase iota.	Biochem. Biophys. Res. Commun.	351	306-311	2006
Fang Z, Duthoit N, Wicher G, Kallskog O, Ambartsumian N, Lukanidin E, Takenaga K, Kozlova EN.	Intracellular calcium-binding protein S100A4 influences injury-induced migration of white matter astrocytes.	Acta Neuropathol. (Berl).	111	213-219	2006
Fang Z, Forslund N, Takenaga K, Lukanidin E, Kozlova EN.	Sensory neurite outgrowth on white matter astrocytes is influenced by intracellular and extracellular S100A4 protein.	J. Neurosci. Res.	83	619-626	2006

Takano-Maruyama M, Hase K, Fukamachi H, Kato Y, Koseki H, Ohno H.	Foxl1-deficient mice exhibit aberrant epithelial cell positioning due to dysregulated EphB/EphrinB expression in the small intestine	Am. J. Physiol. Gastrointest Liver Physiol.	291	G163-170	2006
Blewitt M E, Vickaryous N K , Paldi A, Koseki H, Whitelaw E.	Dynamic reprogramming of DNA methylation at an epigenetically sensitive allele in mice	PLoS Genet	2	e49	2006
Lee T I, Jenner R G., Boyer L A, Guenther M G, Levine S S, Kumar R M, Chevalier B, Johnstone S E, Cole M F, Isono K, Koseki H, Fuchikami T, Abe K, Murray H L, Zucker J P, Yuan B, Bell G W, Herbolsheimer E, Hannett N M, Sun K, Odom D T, Volkert T L, Bartel D P, Melton D A, Gifford D K, Jaenisch R, Young R A.	Control of Developmental Regulators by Polycomb in Human Embryonic Stem Cells	Cell	125	301-313	2006
Fujimura Y, Isono K, Vidal M, Endoh M, Kajita H, Mizutani-Koseki Y, Takihara Y, van Lohuizen M, Otte A, Jenuwein T, Deschamps J, Koseki H.	Distinct roles of Polycomb group gene products between transcriptionally repressed and active domains of Hoxb8.	Development	133	2371-2381	2006
Aikawa Y, Nguyen LA, Isono K, Takakura N, Tagata Y, Schmitz M L, Koseki H, Kitabayashi I.	Roles of HIPK1 and HIPK2 in AML1- and p300-dependent transcription, hematopoiesis and blood vessel formation.	EMBO J.	25	3955-3965	2006
Jorgensen H F, Giadrossi S, Casanova M, Endoh M, Koseki H, Brockdorff N, Fisher A G.	Stem cells primed for action: polycomb repressive complexes restrain the expression of lineage-specific regulators in embryonic stemcells.	Cell Cycle	5	1411-1414	2006
Sato T, Endoh M, Yoshida H, Yasuo S, Katsuno T, Saito Y, Isono K, Koseki H.	Mammalian Polycomb complexes are required for Peyer's patch development by regulating lymphoid cell proliferation.	Gene	379	166-174	2006

Nakayama M, Iida M, Koseki H, Ohara O.	A gene-targeting approach for functional characterization of KIAA genes encoding extremely large proteins.	FASEB J.	20	1718-1720	2006
Schoeftner S, Sengupta A K, Kubicek S, Mechtler K, Spahn L, Koseki H, Jenuwein T, Wutz A.	Recruitment of PRC1 function at the initiation of X inactivation independent of PRC2 and silencing.	EMBO J.	25	3110-3122	2006
Nakajima Y, Morimoto M, Takahashi Y, Koseki H, Saga Y.	Identification of Epha4 enhancer required for segmental expression and the regulation by Mesp2.	Development	133	2517-2525	2006
Hosokawa H, Kimura M Y, Shinnakasu R, Suzuki A, Miki T, Koseki H, van Lohuizen M, Yamashita M, Nakayama T.	Regulation of Th2 Cell Development by Polycomb Group Gene bmi-1 through the Stabilization of GATA3.	J. Immunol.	177	7656-7664	2006
Ogino J, Sakurai K, Yoshiwara K, Suzuki Y, Ishizuka N, Seki N, Suzuki Y, Koseki H, Shirasawa T, Hashimoto N, Yagui K, Saito Y.	Insulin resistance and increased pancreatic beta-cell proliferation in mice expressing a mutant insulin receptor (P1195L).	J. Endocrinol.	190	739-747	2006
Abe M, Westermann F, Nakagawara A, Takato T, Schwab M, Ushijima T.	Marked and independent prognostic significance of the CpG island methylator phenotype in neuroblastomas.	Cancer Lett.	247	253-258	2007
Kaneko S, Ohira M, Nakamura Y, Isogai E, Nakagawara A, Kaneko M.	Relationship of DDX1 and NAG gene amplification/overexpression to the prognosis of patients with MYCN-amplified neuroblastoma.	J. Cancer Res. Clin. Oncol.	133	185-192	2007
Antonelli A, Lenzi L, Nakagawara A, Ozaki T, Chiaretti A, Aloe L.	Tumor suppressor proteins are differentially affected in human ependymoblastoma and medulloblastoma cells exposed to nerve growth factor.	Cancer Investigation	25	1-6	2007

Yamamoto H, Ozaki T, Nakanishi M, Kikuchi H, Yoshida K, Horie H, Kuwano H, Nakagawara A.	Oxidative stress induces p53-dependent apoptosis in hepatoblastoma cell through its nuclear translocation.	Genes to Cells	12	461-471	2007
Nakamura Y, Ozaki T, Niizuma H, Ohira M, Kamijo T, Nakagawara A.	Functional characterization of a new p53 mutant generated by homozygous deletion in a neuroblastoma cell line.	Biochem. Biophys. Res. Commun.	354	892-898	2007
Takahashi M, Ozaki T, Takahashi A, Miyauchi M, Ono S, Takada N, Koda T, Todo S, Kamijo T, Nakagawara A.	DFF45/ICAD restores cisplatin-induced nuclear fragmentation but not DNA cleavage in DFF45-deficient neuroblastoma cells.	Oncogene	In press		2007
Nakanishi H, Ozaki T, Nakamura Y, Hashizume K, Iwanaka T, Nakagawara A.	Purification of human primary neuroblastomas by magnetic beads and their in vitro culture.	Oncology Rep.	In press		2007
Takenaga K, Nygren J, Zelenina M, Ohira M, Iuchi T, Lukanidin E, Sjoquist, M, Kozlova EN.	Modified expression of S100A4/Mts1 protein in C6 glioma cells or surrounding astrocytes affects migration of tumor cells in vitro and in vivo.	Neurobiol Dis.	25	455-463	2007
Nakajima M, Ogawa M, Shimoda Y, Koseki H, Shirasawa T, Furukawa K.	Accelerated acquisition of permeability barrier function in the skin of presenilin-1-deficient embryos.	Arch. Dermatol. Res.	298	339-345	2007
Matsuki Y, Ohmura-Hoshino M, Goto E, Aoki M, Mito-Yoshida M, Uematsu M, Hasegawa T, Koseki H, Ohara O, Nakayama M, Toyooka K, Matsuoka K, Hotta H, Yamamoto A, Ishido S.	Novel regulation of MHC class II function in B cells.	EMBO J.	26	846-854	2007

Takada Y, Isono K, Shinga J, Turner J M, Kitamura H, Ohara O, Watanabe G, Singh P B, Kamijo T, Jenuwein T, Burgoyne P S, Koseki H.	Mammalian Polycomb Scmh1 mediates exclusion of Polycomb complexes from the XY body in the pachytene spermatocytes.	Development	134	579-590	2007
Negishi M, Saraya A, Miyagi S, Nagao K, Inagaki Y, Nishikawa M, Tajima S, Koseki H, Tsuda H, Takasaki Y, Nakauchi H, Iwama A.	Bmi1 cooperates with Dnmt1-associated protein 1 in gene silencing.	Biochem. Biophys. Res. Commun.	353	992-998	2007
Dietrich N, Bracken A P, Trinh E, Schjerling C K, Koseki H, Rappsilber J, Helin K, Hansen KH.	Bypass of senescence by the polycomb group protein CBX8 through direct binding to the INK4A-ARF locus.	EMBO J.	26	1637-1648	2007
Kato Y, Koseki H, Vidal M, Nakauchi H, Iwama A.	Unique composition of polycomb repressive complex 1 in hematopoietic stem cells.	Int. J. Hematol.	85	179-181	2007

Ⅳ. 研究成果の刊行物・別刷

Oncogene (2006) 25, 917–928

www.nature.com/onc

ORIGINAL ARTICLE

Hypoxia selects for high-metastatic Lewis lung carcinoma cells overexpressing Mcl-1 and exhibiting reduced apoptotic potential in solid tumors

N Koshikawa[1,2], C Maejima[1], K Miyazaki[3], A Nakagawara[3] and K Takenaga[1]

[1]Division of Chemotherapy, Chiba Cancer Center Research Institute, Chuoh-ku, Chiba, Japan; [2]Division of Pathology, Chiba Cancer Center Research Institute, Chuoh-ku, Chiba, Japan and [3]Division of Biochemistry, Chiba Cancer Center Research Institute, Chuoh-ku, Chiba, Japan

Low oxygen tension (hypoxia) is a common feature of solid tumors and stimulates the expressions of a variety of genes including those related to angiogenesis, apoptosis and endoplasmic reticulum (ER) stress response. Here we show a close correlation between metastatic potential and the resistance to hypoxia- and ER stress-induced apoptosis among the cell lines with differing metastatic potential derived from Lewis lung carcinoma. An apoptosis-specific expression profiling and immunoblot analyses revealed that the expression of antiapoptotic Mcl-1 increased as the resistance to apoptosis increased. Downregulation of the Mcl-1 expression in the high-metastatic cells by Mcl-1 small interfering RNA increased the sensitivity to hypoxia-induced apoptosis and decreased the metastatic ability. The hypoxia-induced apoptosis was not associated with p53 accumulation, although at present it is not possible to conclude that apoptosis-induced apoptosis is p53-independent. There was no correlation between the expression levels of ER stress-response proteins GADD153, GRP78 and ORP150 and the resistance to hypoxia or ER stresses. *In vitro*, small numbers of the high-metastatic cells overtook the low-metastatic cells after exposure to several rounds of hypoxia and reoxygenation. In solid tumors initially established from equal mixtures, the proportion of the high-metastatic cells to low-metastatic cells was significantly higher in hypoxic areas. Moreover, the high-metastatic cells were overtaking the low-metastatic cells in some of the tumors. Thus, tumor hypoxia and ER stress may provide a physiological selective pressure for the expansion of the high-metastatic cells overexpressing Mcl-1 and exhibiting reduced apoptotic potential in solid tumors.
Oncogene (2006) **25**, 917–928. doi:10.1038/sj.onc.1209128; published online 10 October 2005

Keywords: hypoxia; ER stress; apoptosis; Mcl-1; metastasis

Correspondence: Dr K Takenaga, Division of Chemotherapy, Chiba Cancer Center Research Institute, 666-2 Nitona, Chuoh-ku, Chiba 260-8717, Japan.
E-mail: keizo@chiba-cc.jp
Received 6 January 2005; revised 22 August 2005; accepted 22 August 2005; published online 10 October 2005

Introduction

Response to low oxygen tension (hypoxia) is a fundamental biological phenomenon and therefore hypoxia gives rise to a variety of physiological responses at cellular, local and systemic levels. The cells placed under hypoxic conditions activate many genes including those related to cell survival, glycolysis, angiogenesis, erythrocyte production and iron metabolism to adapt the environment (Semenza, 2000, 2002; Harris, 2002). The oxygen sensing mechanisms have been intensively studied and found to involve hypoxia-inducible factors (HIFs) as key regulatory transcription factors that are composed of HIF-α subunit and HIF-β/aryl hydrocarbon receptor nuclear translocator subunit (Semenza, 2000, 2002; Harris, 2002). HIF binds to the hypoxia-responsive element of hypoxia-responsive genes such as vascular endothelial growth factor (VEGF) and proapoptotic Bnip3, a member of the Bcl-2 family (Semenza, 2000, 2002; Harris, 2002).

Most solid tumors harbor areas of hypoxia, both acute and chronic, due to aberrant vasculature formation and high interstitial pressure (Chaplin and Hill, 1995; Brown and Giaccia, 1998). Although most of the tumor cells die in chronic hypoxia, some of them actually can survive for more than several days in a quiescent or the so-called dormant state (Durand and Sham, 1998) and restart to divide once closed vessels reopen or new vasculatures reach the hypoxic areas. It has been shown that hypoxia induces genetic instability, DNA over-replication and gene amplification in a variety of cultured cells (Rice *et al.*, 1986; Russo *et al.*, 1995; Coquelle *et al.*, 1998). A short-term hypoxia followed by reoxygenation transiently enhances invasive and metastatic potential of some tumor cells (Young and Hill, 1990; Graham *et al.*, 1999; Cairns *et al.*, 2001). Tumor hypoxia selects $p53^{-/-}$ transformed cells and thereby expands cells with diminished apoptotic potential *in vitro* (Graeber *et al.*, 1996). These mechanisms all together are likely to influence the malignant progression of tumor cells (Hill, 1990; Russo *et al.*, 1995; Graeber *et al.*, 1996; Coquelle *et al.*, 1998; Dachs and Chaplin, 1998). Besides, since hypoxic tumor cells cease to divide, they are resistant to conventional radiotherapy and chemotherapy (Rice *et al.*, 1986; Young and Hill, 1990; Teicher, 1994).

Physiological endoplasmic reticulum (ER) stress such as glucose starvation is also present in solid tumors. Hypoxia has been shown to upregulate ER stress-response genes including growth arrest/DNA damage-inducible protein 153 (GADD153/CHOP), which is a proapoptotic transcription factor (Friedman, 1996) and ER chaperones such as glucose-regulated protein (GRP)78/BIP (Munro and Pelham, 1986) and oxygen-regulated protein (ORP)150, which are antiapoptotic proteins (Kuwabara *et al.*, 1996). Upregulation of these ER stress proteins is HIF-independent.

There is accumulating evidence that developing resistance to common apoptotic stimuli is one of the factors that confer high metastatic capability to tumor cells (Glinsky and Glinsky, 1996; McConkey *et al.*, 1996; Bufalo *et al.*, 1997; Glinsky, 1997; Inbal *et al.*, 1997; Shtivelman, 1997; Takaoka *et al.*, 1997; Fernandez *et al.*, 2000; Lowe and Lin, 2000; Wong *et al.*, 2001). The apoptosis-resistant phenotype may be advantageous for tumor cells to survive in the metastatic process. We reported that the high-metastatic clone (A11 cells) established from Lewis lung carcinoma is more resistant to apoptosis induced by serum starvation, hypoxia and glucose deprivation than the low-metastatic clone (P29 cells) (Takasu *et al.*, 1999). However, it remained to be examined whether there is a correlation between metastatic ability and resistance to apoptosis induced by various stresses among various clones with differing metastatic potential. In addition, molecular mechanisms of the apoptosis resistance of the high-metastatic cells remained obscure. We addressed here these points and, furthermore, if hypoxia could act as a physiological selective pressure in solid tumors for the expansion of high-metastatic tumor cells that possess diminished apoptotic potential. The results showed that the high-metastatic Lewis lung carcinoma cell lines are more resistant to hypoxia- and ER stress-induced apoptosis than the low-metastatic cell lines, that the high-metastatic cells overexpress antiapoptotic Mcl-1, and that hypoxia selects for the high-metastatic cells in solid tumors.

Results

Correlation between metastatic potential and resistance to hypoxia- and ER stress-induced apoptosis in the low- and high-metastatic cell lines

To investigate the correlation between susceptibility to hypoxia-induced cell death and metastatic potential, we exposed the five cell lines with differing metastatic potential derived from a mouse Lewis lung carcinoma (metastatic capability; P29 = P34 < C2 < D6 < A11) to hypoxia (~0.1% O_2), corresponding to oxygen concentrations commonly found in solid tumors. Cell death was monitored after culturing the cell lines for 72 h under hypoxia. The results showed that only less than 8% of P29 and P34 cells were viable while about 20% of C2 cells and over 45% of D6 and A11 cells remained viable (Figure 1a). Thus, we observed a tendency where the resistance to hypoxia-induced cell death is correlated with the metastatic ability. The time course showed that hypoxia induced cell death more rapidly in P29 cells than in A11 cells (Figure 1b). Clonogenic assays in which the cells were exposed to hypoxia for 3 or 4 days and then reoxygenated to form colonies also demonstrated that A11 cells survived longer than P29 cells under hypoxic conditions (Figure 1c). The cells positive for annexin V and TUNEL staining increased in hypoxic P29 cells (Figure 1d). An increase in the number of cells exhibiting chromatin condensation and fragmentation as assessed by DAPI staining was also observed in hypoxic P29 cells (0.1 and 26.1% for normoxic and hypoxic P29 cells, respectively) (Figure 1d). In addition, flow cytometric analysis revealed an increase in the percentage of sub-G1 population in these cells (0.7 and 20.6% for normoxic and hypoxic cells, respectively) (Figure 1e). Thus, these data indicate that hypoxic P29 cells were dying through apoptosis. We confirmed that hypoxic A11 cells died of apoptosis based on the same criteria.

To test whether the high-metastatic cell lines are also resistant to ER stresses compared with the low-metastatic cell lines, we treated P29, P34, D6 and A11 cells with chemical ER stress inducers for 2 days and examined their viability. As shown in Figure 2, compared to P29 and P34 cells, D6 and A11 cells were much more resistant to apoptosis induced by tunicamycin (5 μg/ml), brefeldin A (5 μg/ml), thapsigargin (250 nM) and A23187 (1 μM).

Mcl-1 is overexpressed in the high-metastatic cell lines

To find out the genes responsible for the susceptibility to hypoxia-induced apoptosis, we compared the expression profile of apoptosis-related genes among normoxic and hypoxic P29 and A11 cells using a cDNA expression microarray cumulated apoptosis-related genes. The data showed that A11 cells expressed antiapoptotic *Mcl-1* gene at higher levels than P29 cells (not shown). Immunoblot analysis confirmed a higher expression of Mcl-1 in A11 cells than in P29 cells under both normoxic and hypoxic conditions (Figure 3A). We detected two close bands (40 and 37 kDa) on the blots. Since the expressions of the bands were decreased by treatment with Mcl-1 siRNA (see below), the 37 kDa band may be a degradation product of Mcl-1 or, though less likely, a splicing variant of *Mcl-1* gene. It is of note that the cell lines expressed Mcl-1 (40 kDa) at the levels according to the resistance to hypoxia- and other stress-induced apoptosis (Figure 3A and B). Consistent with the recent report that hypoxia enhances Mcl-1 expression in hepatoma HepG2 cells through HIF-1 (Piret *et al.*, 2005), the amount of Mcl-1 was increased by hypoxia in C2, D6 and A11 cells (Figure 3B). Immunohistochemistry for Mcl-1 on the sections prepared from paraffin-embedded P29 and A11 tumors showed a higher expression of Mcl-1 in A11 cells than in P29 cells, indicating that Mcl-1 overexpression is persistent even *in vivo* (Figure 3C).

The expression profiling also showed that hypoxia induced proapoptotic *Bnip3* gene expression in both P29

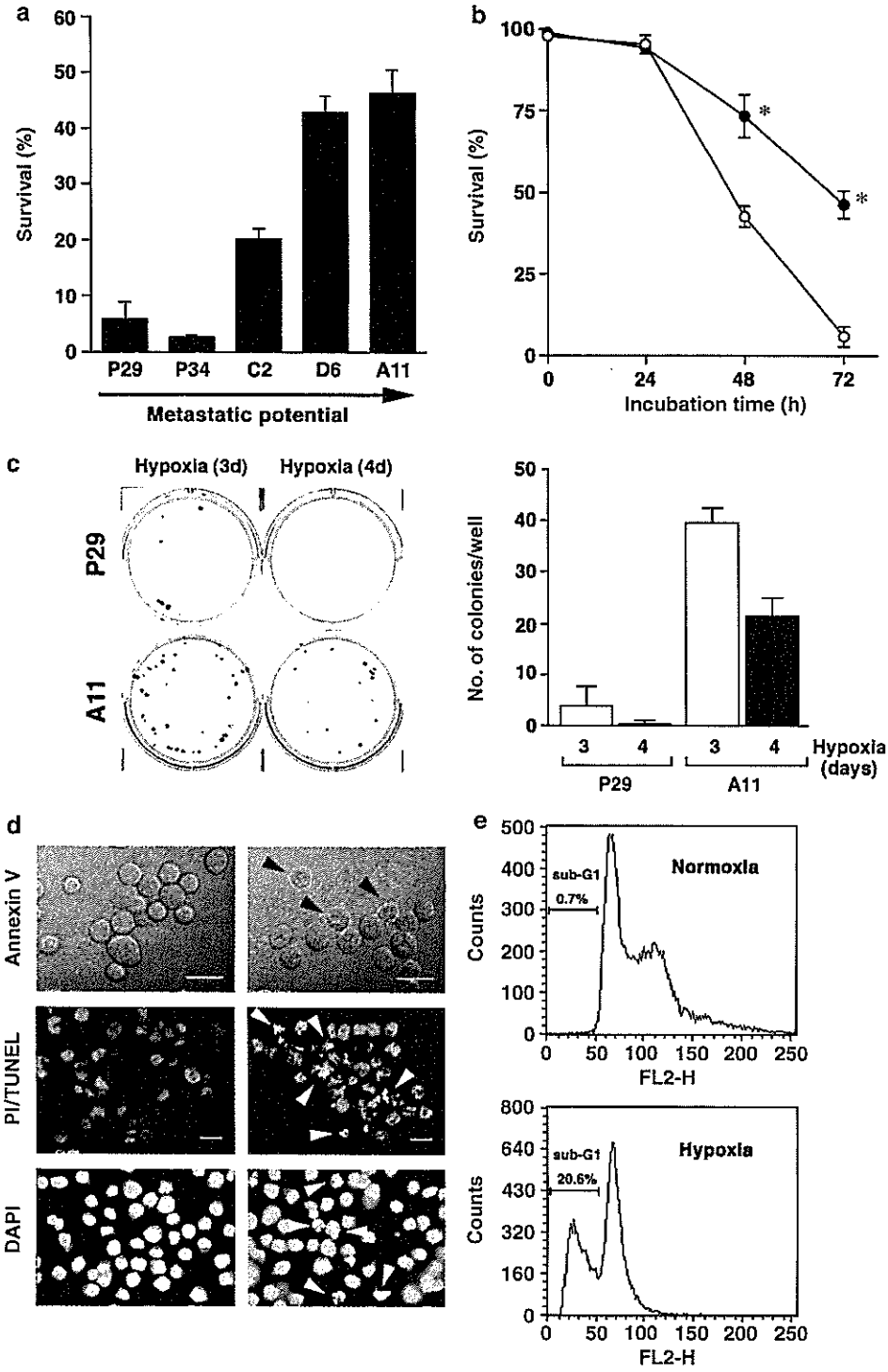

Figure 1 Sensitivity to hypoxia-induced apoptosis of the Lewis lung carcinoma cell lines. (**a**) Hypoxia-induced cell death of the cell lines with differing metastatic potential. The cell lines were exposed to hypoxia for 72 h. Percentage of living cells was determined on the basis of trypan blue exclusion. Bars; s.d. of triplicate determinations. (**b**) Time course of cell death induced by hypoxia. P29 (○) and A11 cells (•) were exposed to hypoxia for the indicated time period. Percentage of living cells was determined on the basis of trypan blue exclusion Bars; s.d. of triplicate determinations. *Significant at $P<0.002$. (**c**) Clonogenic assay of cell survival. P29 and A11 cells (100 cells/well) were cultured under hypoxic conditions for 3 or 4 days followed by culturing under normoxic conditions. Colonies were stained with crystal violet (left panel) and then counted (right panel). Bars; s.d. of triplicate determinations. (**d**) Annexin V, TUNEL and DAPI stainings of normoxic (left panels) and hypoxic P29 cells (right panels). P29 cells were cultured under hypoxic conditions for 18, 27 or 28 h, and then stained for annexin V-EGFP, TUNEL (green) and PI (red), or DAPI, respectively. Arrowheads show apoptotic cells. (**e**) Flow cytometric analysis of DNA fragmentation. P29 cells cultured under hypoxic conditions for 27 h were subjected to FACscan analysis. The percentage of sub-G1 fraction is also shown.

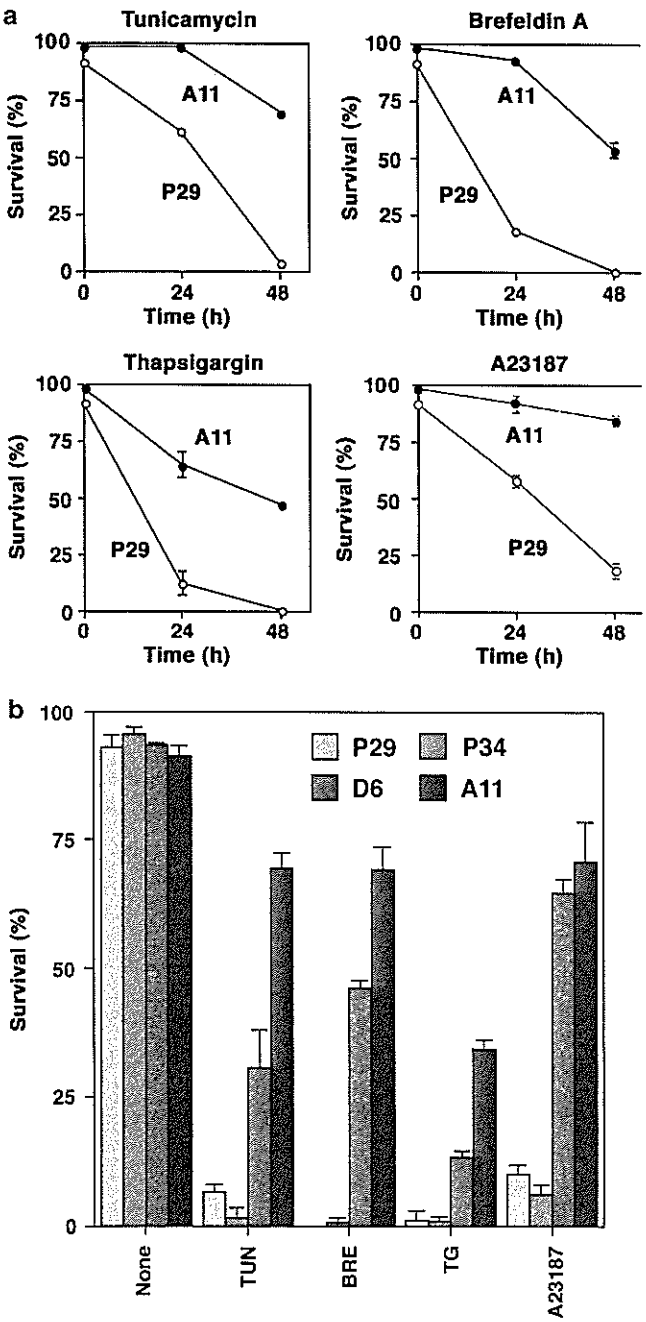

Figure 2 Sensitivity to ER stress-induced apoptosis of the Lewis lung carcinoma cell lines. (a) Time course of cell death of P29 (○) and A11 cells (●) exposed to ER stress-inducing agents. The cells were exposed to tunicamycin (5 μg/ml), brefeldin A (5 μg/ml), thaspigargin (250 nM), A23187 (1 μM)). (b) Sensitivity of the cell lines with differing metastatic potential to ER stress-inducing agents. P29, P34, D6 and A11 cells were exposed to tunicamycin (5 μg/ml), brefeldin A (5 μg/ml), thaspigargin (250 nM), A23187 (1 μM)) for 2 days. Percentage of living cells was determined on the basis of trypan blue exclusion. Bars; s.d. of triplicate determinations.

and A11 cells (data not shown). Actually, *Bnip3* mRNA expression was induced in all of the cell lines, but the expression level was not correlated with the susceptibility to hypoxia- and other stress-induced apoptosis (Figure 3D).

To investigate whether the hypoxia-induced apoptosis is associated with p53 accumulation, we examined the expression of p53 in hypoxia- and doxorubicin-treated P29, P34, D6 and A11 cells. Immunoblot analysis revealed that hypoxia reduced p53 expression (Figure 3E) and failed to induce endogenous downstream p53 effector proteins, Bax and $p21^{WAF1/CIP1}$, in these cell lines (not shown). By contrast, doxorubicin caused the accumulation of p53 (Figure 3E).

We next compared the expression levels of ER stress-response proteins, GADD153, GRP78 and ORP150, which are known to be induced by hypoxia, between P29 and A11 cells. As shown in Figure 3F and G, the expressions of these proteins were induced by tunicamycin and hypoxia, but there was no difference between 29 and A11 cells.

Effects of Mcl-1 siRNA on hypoxia-induced apoptosis and metastatic potential

To examine if the expression of Mcl-1 is responsible for the resistance to hypoxia-induced apoptosis, we transfected A11 cells with either Mcl-1 siRNA or control siRNA. As shown in Figure 4a and b, the expression of Mcl-1 was suppressed by Mcl-1 siRNA, but not by control siRNA. We then cultured these cells under hypoxic conditions for 60 h and monitored cell death. The results showed that Mcl-1 siRNA-treated A11 cells were more sensitive to hypoxia-induced apoptosis than mock and control siRNA-treated cells in both normal growth medium and serum-starved medium (Figure 4c). Importantly, Mcl-1 siRNA-treated A11 cells were less metastatic than control siRNA-treated cells, as assessed by lung weight and the number of metastatic nodules in the lung (Figure 4d). Thus, it appeared that Mcl-1 is at least in part involved in resistance to hypoxia-induced apoptosis and metastatic potential of A11 cells.

Apoptosis of the low- and high-metastatic cells in hypoxic areas of solid tumors

To examine whether the difference in the susceptibility to hypoxia-induced apoptosis can also be observed *in vivo*, we injected EF5, a nitroimidazole compound, into mice bearing subcutaneous P29 or A11 tumors of nearly equal size for detecting hypoxic areas and stained cryosections of the tumors first with TUNEL assay using fluorescein-labeled nucleotides, and then with Cy3-labeled antibodies against EF5-cellular macromolecule adducts (Figure 5a). EF5 binding occurs under low-oxygen conditions and only in viable cells (Lord *et al.*, 1993). The number of TUNEL-positive cells per 100 μm^2 in EF5-positive (hypoxic) and -negative (normoxic) areas was counted (Figure 5b). We omitted necrotic areas from the investigation. The results showed that the number of apoptotic cells in hypoxic areas of P29 tumors was fourfold larger than that in hypoxic areas of A11 tumors. In normoxic areas, the number of apoptotic cells was small but statistically larger in P29 tumors than in A11 tumors.

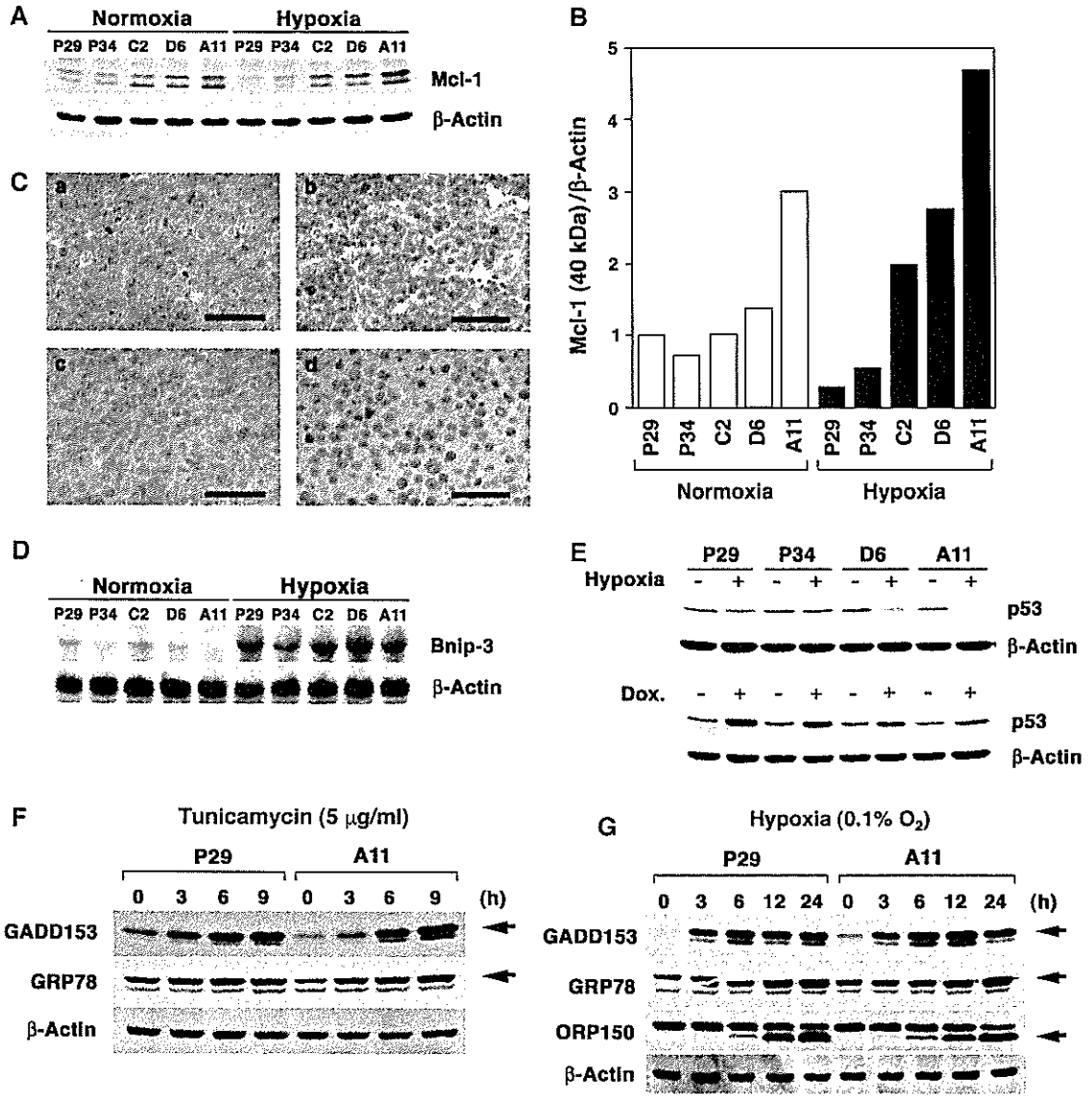

Figure 3 Expressions of apoptosis-related genes in Lewis lung carcinoma cell lines. (A) Western blot analysis of the effect of hypoxia on Mcl-1 expression. The cells exposed to hypoxia (~0.1% O_2) for 8 h were subjected to immunoblot analysis for Mcl-1 expression. β-actin served as loading controls. (B) Relative values for signal intensity of Mcl-1 (40 kDa) after normalization to the level of β-actin. Scanning densitometry of the gel was performed and the normalized values were represented by the white (under normoxia) and black (under hypoxia) bars. All values are shown as a percentage of the value for normoxic P29 cells. The results are representative of two separate experiments in which similar results were obtained. (C) Immunohistochemical analysis of Mcl-1 expression in P29 and A11 tumors. Sections from P29 tumors (a and c) and A11 tumors (b and d) were immunostained with anti-Mcl-1 antibody (a and b) and control IgG (c and d). Bars; 50 μm. (D) Effects of hypoxia on *Bnip3* mRNA expression. The cells exposed to hypoxia (0.1% O_2) for 8 h were subjected to Northern analysis for Bnip3 mRNA expression. β-Actin mRNA served as loading controls. (E) Western blot analysis of the effects of hypoxia and doxorubicin on the accumulation of p53 protein. The cells exposed to hypoxia (0.1% O_2) for 24 h or 5 μg/ml doxorubicin (Dox) for 20 h were subjected to immunoblot analysis for p53 expression. β-Actin served as loading controls. (F) Western blot analysis of the effects of tunicamycin on the expressions of GADD153 and GRP78. P29 and A11 cells were exposed to 5 μg/ml tunicamycin for the indicated periods of time. βActin served as loading controls. (G) Western blot analysis of the effects of hypoxia on the expressions of GADD153, GRP78 and ORP150. P29 and A11 cells were exposed to hypoxia (0.1% O_2) for the indicated periods of time. β-actin served as loading controls.

Survival advantage of the high-metastatic cells under hypoxic conditions

The above results prompted us to examine whether A11 cells have a survival advantage over P29 cells under hypoxic conditions. To this end, we established genetically labeled P29 ($P29^{EGFP}$ cells) and A11 cells ($A11^{IRES\text{-}EGFP}$ cells) after selecting P29 and A11 cells stably transfected with pEGFP-N1 and pIRES2-EGFP, respectively (Figure 6a), and characterized their properties. $P29^{EGFP}$ cells grew faster than $A11^{IRES\text{-}EGFP}$ cells *in vivo*, and at 17 days after tumor cell inoculation $P29^{EGFP}$ tumors were twice larger than $A11^{IRES\text{-}EGFP}$ tumors (Figure 6b). $P29^{EGFP}$ tumors contained large necrotic regions. $P29^{EGFP}$ and $A11^{IRES\text{-}EGFP}$ cells were low- and

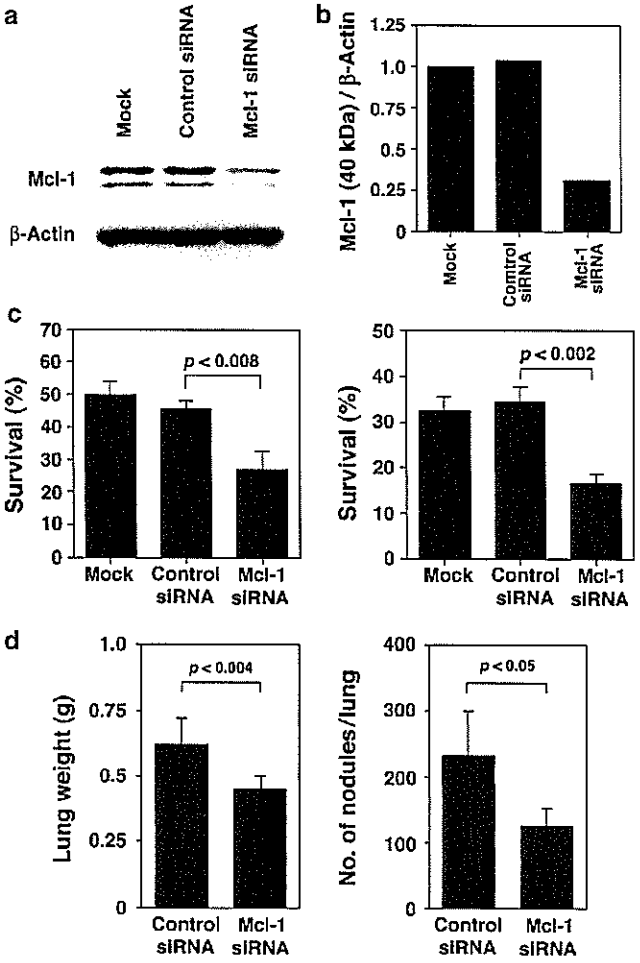

Figure 4 Effects of Mcl-1 siRNA on hypoxia-induced apoptosis and metastatic potential of A11 cells. (**a**) Expression of Mcl-1 in A11 cells treated with Mcl-1 siRNA. A11 cells pretreated with Lipofectamine 2000 alone (mock), 25 nM control siRNA or 25 nM Mcl-1 siRNA for 2 days were subjected to immunoblot analysis for Mcl-1 expression. β-Actin served as loading controls. (**b**) Relative values for signal intensity of Mcl-1 (40 kDa) after normalization to the level of β-actin. Scanning densitometry of the gel was performed and the relative values were represented. All values are shown as a percentage of the value for mock-transfected A11 cells. The results are representative of three separate experiments in which similar results were obtained. (**c**) Sensitivity of Mcl-1 siRNA-treated A11 cells to hypoxia-induced apoptosis. A11 cells pretreated with Lipofectamine 2000 alone (mock), 25 nM control siRNA or 25 nM Mcl-1 siRNA for 2 days were cultured under hypoxic conditions (~0.1% O_2) for 60 h in normal growth medium (left panel) or serum-starved (1% serum) medium (right panel). Cell death was examined by trypan blue staining. Bars; s.d. of triplicate determinations. (**d**) Metastatic potential of Mcl-1 siRNA-treated A11 cells. A11 cells pretreated with 25 nM control siRNA or 25 nM Mcl-1 siRNA for 2 days were injected intravenously into C57BL/6 mice (6 mice/group). At 17 days after the injection, the weight of the lungs (left panel) and the number of metastatic nodules (right panel) were measured. Bars; s.d.

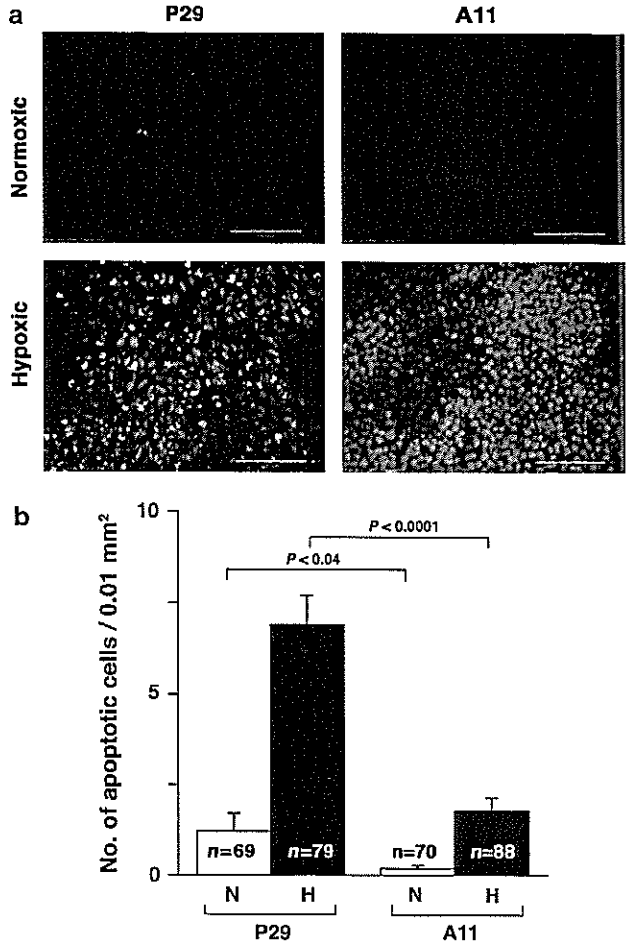

Figure 5 Apoptosis of P29 and A11 cells in tumor hypoxic areas. (**a**) TUNEL staining (green) and EF5 staining (red) of frozen sections of subcutaneous tumors established from P29 and A11 cells. (**b**) Frequency of apoptotic (TUNEL-positive) cells in normoxic (N) and hypoxic (H) areas. Bars; s.e.m.

high-metastatic, respectively, in both experimental and spontaneous metastasis assays (Figure 6c) and showed a similar apoptosis resistance to their parental cells (Figure 6d).

To obtain a standard curve by which the percentage of $A11^{IRES\text{-}EGFP}$ cells in mixtures of unknown proportions of $P29^{EGFP}$ and $A11^{IRES\text{-}EGFP}$ cells could be calculated, we extracted genomic DNA from mixtures of known proportions of the cells and performed PCR followed by Southern blot with an EGFP probe (Figure 6e). By plotting the relative intensities of the bands corresponding to EGFP and IRES-EGFP against the known proportion of $A11^{IRES\text{-}EGFP}$ cells, a standard curve, although slightly sigmoid, was obtained (Figure 6f). The value at each point did not significantly fluctuate even when we carried out PCR under various conditions (1–100 ng DNA, 20–35 PCR cycles) (not shown).

We then mixed $A11^{IRES\text{-}EGFP}$ and $P29^{EGFP}$ cells at a 1:1, 1:10 or 1:100 ratio and treated them with multiple rounds of hypoxia and reoxygenation (recovery in normoxia). The percentage of $A11^{IRES\text{-}EGFP}$ cells at the time of cell harvesting was determined from the standard curve after quantitation of radioactive intensity of the PCR bands. We found that the percentage of $A11^{IRES\text{-}EGFP}$ cells increased dramatically after several rounds of hypoxia-reoxygenation in every case (Figure 7a and b). The intensity of the band corresponding to EGFP and IRES-EGFP in $P29^{EGFP}$ and $A11^{IRES\text{-}EGFP}$

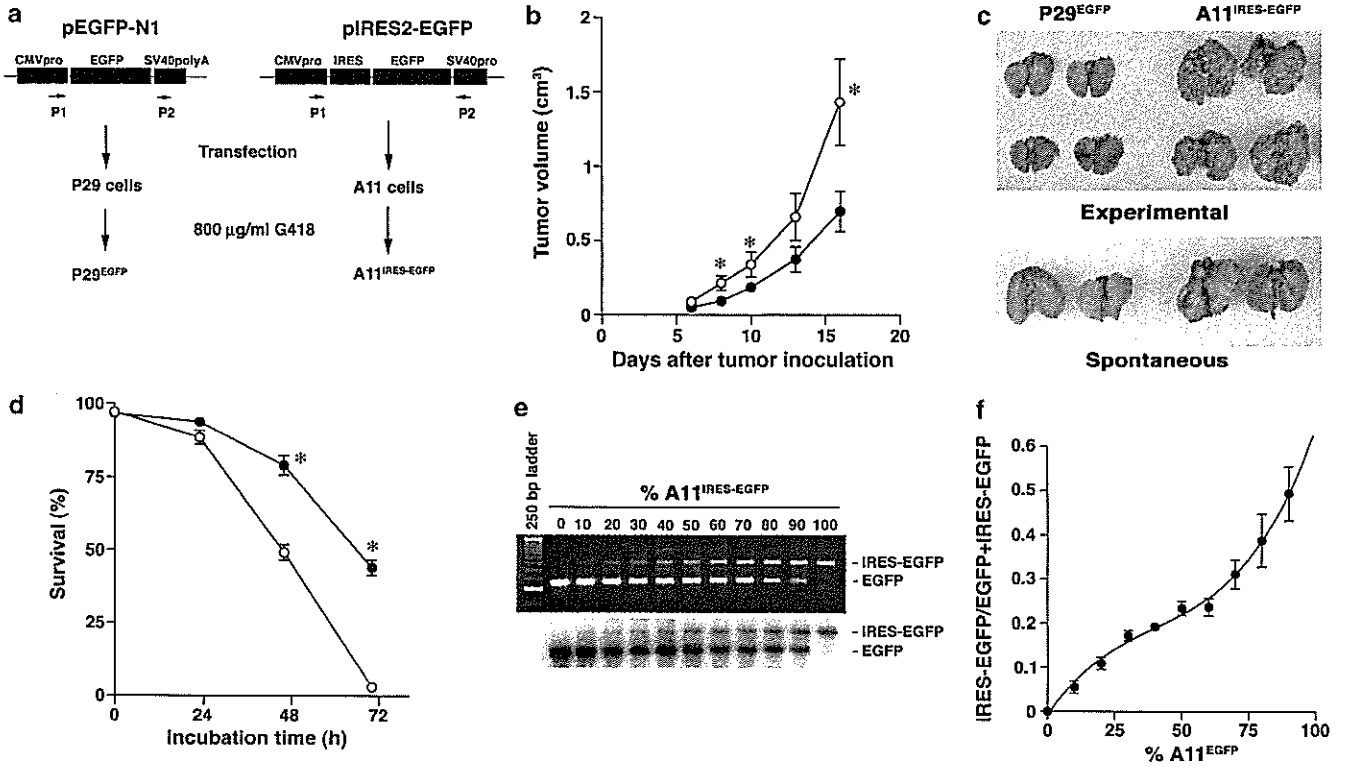

Figure 6 Establishment and properties of $P29^{EGFP}$ and $A11^{IRES\text{-}EGFP}$ cells. (a) Schematic drawings of the establishment of $P29^{EGFP}$ and $A11^{IRES\text{-}EGFP}$ cells and the primers, P1 and P2, used for PCR. (b) *In vivo* growth of $P29^{EGFP}$ and $A11^{IRES\text{-}EGFP}$ cells. $P29^{EGFP}$ (○) and $A11^{IRES\text{-}EGFP}$ cells (•) (2.5×10^5) were injected subcutaneously into C57BL/6 mice (7 mice/group). Bars; s.e.m. *Significant at $P<0.04$. (c) Metastatic potential of $P29^{EGFP}$ and $A11^{IRES\text{-}EGFP}$ cells. For experimental metastasis, the cells (2×10^5 cells/mouse) were injected intravenously, and the lungs were excised 17 days after the injection. For spontaneous metastasis, the cells (2×10^5 cells/mouse) were inoculated subcutaneously, and the lungs were excised 30 days after the inoculation. (d) Hypoxia-induced apoptosis of $P29^{EGFP}$ (○) and $A11^{IRES\text{-}EGFP}$ cells (•). Percentage of living cells was determined on the basis of trypan blue exclusion. Bars; s.d. of triplicate determinations. *Significant at $P<0.003$. (e) Ethidium bromide staining and Southern blot of PCR fragments amplified using genomic DNA extracted from mixtures of known proportions of $P29^{EGFP}$ and $A11^{IRES\text{-}EGFP}$ cells. (f) A standard curve by which the percentage of $A11^{IRES\text{-}EGFP}$ cells in a mixed culture or a tumor could be calculated. The relative intensities of the bands shown in (e) were plotted against the known proportion of $A11^{IRES\text{-}EGFP}$ cells. Bars; s.d. of three independent experiments.

cells, respectively, treated with the same protocol was constant (Figure 7c), indicating that the integrated marker genes was stable.

Survival advantage of the high-metastatic cells in solid tumors

We next examined the proportion of $A11^{IRES\text{-}EGFP}$ cells in normoxic and hypoxic areas of solid tumors established from a 1:1 mixture of $P29^{EGFP}$ and $A11^{IRES\text{-}EGFP}$ cells. Since $P29^{EGFP}$ cells grew faster than $A11^{IRES\text{-}EGFP}$ cells *in vivo* (Figure 6b), the percentage of $A11^{IRES\text{-}EGFP}$ cells in both normoxic and hypoxic areas of the heterogeneous tumors should be lower than 50% if no selection of cells occurs in the tumors. We cut out EF5-negative and -positive areas (approximately total 1 mm^2) from cryosections of the tumors excised at 17 days after tumor inoculation by using laser-assisted microdissection, extracted genomic DNA, and then examined the percentage of $A11^{IRES\text{-}EGFP}$ cells in these areas as described above (Figure 8a and b). The data showed that the proportion of $A11^{IRES\text{-}EGFP}$ cells in normoxic areas decreased from the initial 50% in five out of the seven mixed tumors. However, the proportion was over 70% in #2 and #5 tumors (Figure 8b). Intriguingly, the percentage of $A11^{IRES\text{-}EGFP}$ cells in hypoxic areas was quite high in five out of the seven tumors. Overall, the proportion of $A11^{IRES\text{-}EGFP}$ cells in normoxic and hypoxic areas was 36.4 ± 26.0 and $69.0 \pm 21.0\%$, respectively ($P<0.011$). The intensity of bands corresponding to EGFP and IRES-EGFP of the cells collected from normoxic and hypoxic areas of $P29^{EGFP}$ and $A11^{IRES\text{-}EGFP}$ tumors was constant (Figure 8c), indicating that the integrated marker genes was also stable *in vivo*. Thus, $A11^{IRES\text{-}EGFP}$ cells showed a clear survival advantage over $P29^{EGFP}$ cells in hypoxic areas.

The loss of $P29^{EGFP}$ cells in normoxic areas of some heterogeneous tumors (#2 and #5 tumors) suggests a possibility that a greater portion of $P29^{EGFP}$ cells was lost in the tumors. To test this possibility, we extracted genomic DNA from the whole tumors and examined the proportion of $A11^{IRES\text{-}EGFP}$ cells. The results showed that the proportion was over 90% in #2 tumor, indicating that $A11^{IRES\text{-}EGFP}$ cells nearly overtook $P29^{EGFP}$ cells in this tumor (Figure 8d and e). In #5 tumor, it was below 50%. This and the above results suggest that $A11^{IRES\text{-}EGFP}$